JOURNAL OF PHYSICAL ORGANIC CHEMISTRY
J. Phys. Org. Chem. 2005; **18:** 1–8

Kinetic isotope effects for non-adiabatic proton transfer in benzophenone–*N*-methylacridan contact radical ion pairs

Kevin S. Peters* and Ganghyeok Kim

Department of Chemistry and Biochemistry, University of Colorado, Boulder, Colorado 80309-0215, USA

Received 23 February 2004; revised 23 June 2004; accepted 24 June 2004

ABSTRACT: The dynamics of proton transfer within a variety of substituted benzophenones–*N*-methylacridan contact radical ion pairs in benzene were examined. The correlation of the rate constants for proton transfer with the thermodynamic driving force reveals both normal and inverted regions for proton transfer in benzene. Employing the isotopically labeled compounds *N*-methyl-d_3-acridan and *N*-methylacridan-9,9-d_2, the kinetic deuterium isotope effects were examined. The isotope dependence for the transfer process was examined within the context of the Lee–Hynes model for non-adiabatic proton transfer. The theoretical analysis of the experimental data suggests that the reaction path for proton–deuteron transfer involves tunneling. Conventional transition-state theory with the inclusion of the Bell correction for tunneling in the region of the transition state cannot account for the observed kinetic behavior. Copyright © 2004 John Wiley & Sons, Ltd.

KEYWORDS: kinetic isotope effects; non-adiabatic proton transfer; contact radical ion pairs; benzophenone; *N*-methylacridan

INTRODUCTION

A common reaction in the chemistry of organic cation radicals involves the loss of a proton from the carbon acid, generating a neutral radical species.[1] Thus, the mechanism by which a proton is transferred continues to be the subject of numerous experimental and theoretical studies.[2–20] The standard theoretical framework for the analysis of the associated reaction dynamics is transition-state theory modified to include the Bell tunneling correction in the region of the transition state.[21–24] However, in recent years, the theoretical assumptions, as they pertain to proton transfer, that underlie transition state theory have been brought into question.[25–35]

The idea that the reaction path for proton transfer does not involve passage through a transition state in the proton transfer coordinate has been in the literature for more than 30 years.[25,26] Kuznetzov and co-workers proposed that when the transferring proton encounters an electronic barrier in the transfer reaction coordinate, the proton tunnels through the electronic barrier into the product state leading to a non-adiabatic process. To achieve the required resonance condition for tunneling, it is the fluctuation in the solvent structure that brings the reactant and product states into resonance that is integral in determining the overall reaction dynamics.[25,26] Numerous theoretical studies have since advanced these initial theoretical models for non-adiabatic proton transfer. Notably, Borgis and co-workers revealed the importance of low-frequency vibrational modes in enhancing the rates of proton tunneling.[27–30] More recently, Hammes-Schiffer and Tully combined these ideas for proton transfer with the theory for electron transfer to develop models for proton-coupled electron transfer reactions.[34,35]

Recently, we reported on a series of experiments that examined the nature of proton transfer in benzophenone–*N*,*N*-dimethylaniline contact radical ion pairs.[17–20] By varying substituents on the 4,4′-positions of benzophenone, the thermodynamic driving force for proton transfer was varied by 10 kcal mol^{-1} (1 kcal = 4.184 kJ) in a variety of non-polar and polar solvents. Correlating the rate constant data with driving force, both normal and inverted regions were observed for proton transfer. The existence of an inverted region was shown to be consistent with non-adiabatic theories for proton transfer and could not be accounted for by theoretical models based on transition-state theory.[17–20] Employing Lee–Hynes theory,[36] a modification of Borgis–Hynes theory that incorporates the activity of various vibrational modes in the product state, both solvent effects and kinetic deuterium isotope effects on the rates of proton transfer were rationalized. These experimental studies strongly support

---

**Correspondence to:* K. S. Peters, Department of Chemistry and Biochemistry, University of Colorado, Boulder, Colorado 80309-0215, USA.
E-mail: kevin.peters@colorado.edu
Contact/grant sponsor: National Science Foundation; *Contact/grant number:* CHE-0408265.

the theoretical models for non-adiabatic proton transfer for this particular molecular systems.

In this paper, we examine the dynamics of proton transfer within a variety of 4,4′-disubstituted benzophenone–*N*-methylacridan contact radical ion pairs in benzene. The mechanism of the photochemically induced hydrogen atom transfer, proceeding by an electron–proton sequential transfer, in the benzophenone–*N*-methylacridan pair has been described previously.[37–39] The 355 nm irradiation of benzophenone in benzene produces the first excited singlet state, S_1, which intersystem crosses to the lowest energy triplet state, T_1, on the time scale of 10 ps. In the presence of 0.3 M *N*-methylacridan, the triplet state is quenched by the transfer of an electron from *N*-methylacridan to benzophenone, producing a triplet contact radical ion pair (CRIP) absorbing at 680 nm, with contributions to the spectrum from both the benzophenone radical anion and the *N*-methyacridan radical cation. Subsequent to electron transfer, a proton is transferred from the *N*-methyl group to produce a triplet contact radical pair (CRP) (Scheme 1).

A particularly interesting feature of this proton transfer process is that the source of the proton is derived from the *N*-methyl group in preference to the 9-position, which would produce the thermodynamically more stable radical. That the proton is derived from the *N*-methyl group and not the 9-position was demonstrated by product analysis employing *N*-methyl-d_3-acridan and *N*-methylacridan-9,9-d_2 in a photochemical study.[38,39] The origin of the kinetically preferred path producing the thermodynamically least stable radical was attributed to the geometric constraints imposed upon the CRIP by the π-stacking of the two aromatic systems, which does not allow for the free rotation of the two aromatic systems relative to one another on the time-scale of proton transfer. As with other aromatic exciplexes, the π-stacking produces a separation of the order of 3.3 Å between to two aromatic systems.[40]

In the ensuing discussion, we present an analysis of the rate of proton transfer within the contact radical ion pair as a function of driving force. We also examine the effect of perdeuteration at the *N*-methyl position and at the 9,9-positions of *N*-methylacridan. The correlation of the rate constants of proton–deuteron transfer with the thermodynamic driving force are examined with the context of Lee–Hynes theory for non-adiabatic proton transfer.

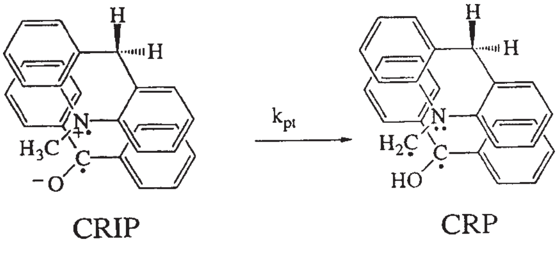

Scheme 1

EXPERIMENTAL

All chemicals were obtained from Aldrich unless noted otherwise. The synthesis of *N*-methylacridan, *N*-methyl-d_3-acridan and *N*-methyacridan-9,9-d_2 has been reported previously.[39] NMR analysis indicated that *N*-methyl-d_3-acridan was >99% d_3-methyl and *N*-methyacridan-9,9-d_2 was >93% d_2.

The picosecond laser absorption spectrometer, employing a Continuum (PY61C-10) Nd:YAG laser producing a 19 ps pulse width, has been described previously.[41] The samples were passed continuously through a 1 cm quartz cuvette. The experiments were undertaken at 23 °C. The photolysis wavelength was 355 nm and the monitoring wavelength, reflecting the time dependence of the benzophenone radical anion and the *N*-methylacridan radical cation, was 680 nm.

For the analysis of the kinetic data with the Lee–Hynes theoretical framework, the vibrational frequencies of the transferring and receiving vibrational modes are required. The vibrational frequencies were calculated employing the perturbative Becke–Perdew model (pBP/DN**) using MacSpartan Pro; the derived values for the vibrational frequencies were scaled by a factor of 0.9.[42]

RESULTS

Determination of free energy change for proton transfer

Central to the analysis for the kinetics of proton transfer is the determination of the free energy change associated with the process. As these energetic changes have not been experimentally determined, it is necessary to estimate them through thermodynamic cycles. The required free energy change is that associated with the decay of the contact radical ion pair through proton transfer to form the triplet radical pair in the solvent benzene (Scheme 1). For the analysis, the reference state is that of the initial ketone–amine reactants. The free energy of the triplet contact radical ion pair, ΔG_{CRIP}, is obtained from the oxidation potential of *N*-methylacridan and the reduction potential of benzophenone through the relationship

$$\Delta G_{\mathrm{CRIP}} = (E_{\mathrm{D}}^{\mathrm{OX}} - E_{\mathrm{A}}^{\mathrm{RED}}) + \Delta_{\mathrm{CRIP}} \qquad (1)$$

where Δ_{CRIP} is the solvent correction based on the Onsager dipole model.[43] The free energy of the triplet radical pair, ΔG_{TPR}, is determined from the enthalpy change associated with the removal of a hydrogen atom from the C—H bond of the *N*-methyl group in *N*-methylacridan and its addition to the triplet state of benzophenone; relative to the initial reactants, the entropy change associated with the formation of the triplet radical pair is assumed to be zero.[18] Thus the free energy change for proton transfer within the benzophenone–*N*-methylacridan contact radical ion pair in benzene is $\Delta G_{\mathrm{TRP}} - \Delta G_{\mathrm{CRIP}}$. Finally, for the various 4,4′-disubstituted benzophenone–*N*-methylacridan contact radical ion pairs, the driving force for proton transfer is estimated through the analysis of the effect that the substituents have on the reduction potential of benzophenone and the effect that the substituents have on the stability of the ketyl radical.[18,44]

For the free energy change associated with the formation of the benzophenone–*N*-methylacridan triplet contract radical ion pair, ΔG_{CRIP}, the reduction potential of benzophenone in acetonitrile is $E_{\mathrm{A}}^{\mathrm{RED}} = -1.86$ V vs SCE.[44] The oxidation potential of *N*-methylacridan in acetonitrile is $E_{\mathrm{D}}^{\mathrm{OX}} = 0.81$ V vs SCE.[45] The solvent correction term Δ_{CRIP} has not been measured or even estimated for the benzophenone–*N*-methylacridan triplet contract radical ion pair. The only determination of Δ_{CRIP} for a contact ion pair to date has been derived from Arnold *et al.*'s study of the solvent dependence of energetics for the contact radical ion pair of 1,2,4,5-tetracyanobenzene–hexmethylbenzene obtained through the analysis of the solvent dependence of their emission spectra.[43] To derive values for Δ_{CRIP} for acetonitrile and for benzene, we have taken their values for Δ_{CRIP} in a variety of solvents and established a correlation with $E_{\mathrm{T}}30$. From this analysis, the value for Δ_{CRIP} for acetonitrile is $+0.6$ kcal mol^{-1} and the value for Δ_{CRIP} for benzene is $+3.7$ kcal mol^{-1}. Thus the free energy change associated with the formation of the benzophenone–*N*-methylacridan triplet contract radical ion pair relative to the ground-state reactants is 65.9 kcal mol^{-1}. Finally, the variation of the free energy of triplet contact ion pair with a change of substituents on 4,4′-benzophenones has been previously discussed, the results of which are given in Table 1.[18]

As previously discussed, the energy of the triplet radial pair is derived from the energy of the triplet state of benzophenone, 69.2 kcal mol^{-1}, the C—H bond dissociation energy of *N*-methylacridan, 91.7 kcal mol^{-1}, and the enthalpy for addition of a hydrogen atom to the benzophenone triplet state, -110.8 kcal mol^{-1}, yielding a free energy for formation of the triplet radical pair relative to initial reactants of 50.1 kcal mol^{-1} where it is again assumed that associated entropy change is negligible.[46,47]

For the transfer of a proton within the contact radical ion pair, the geometric configuration of the reactant state is shown in Scheme 2.

The shortest distance for the tunneling of the proton from the C to O^{-} would produce the conformation of the contact radical pair depicted by CRP 90 (Scheme 2). Based on pBP/DN** calculations, the resulting benzophenone ketyl radical, CRP 90, is a higher energy species relative to CRP 0 so that a 90° rotation of the O—H bond lowers the energy of the ketyl radical by 3.4 kcal mol^{-1}. The preceding estimate of the energy of the triplet radical pair corresponds to the CRP 0 conformation while the reactive state is CRP 90. Therefore, the free energy for the initial product state, CRP 90, is 53.5 kcal mol^{-1}.

Table 1. Triplet state energies for 4,4′-substituted benzophenones, E_{T}, the reduction potential of ketones, *Red*, the free energy change for formation of 4,4′-substituted benzophenone–*N*-methylacridan triplet contact radical ion pair, ΔG_{CRIP}, the free energy change for formation of 4,4′-substituted benzophenone–*N*-methylacridan triplet radical pair, ΔG_{TRP}, and the free energy change for proton transfer, ΔG_{PT} (all values in kcal mol^{-1})

Compound						
4	4′	E_{T}[a]	*Red*[b]	ΔG_{CRIP}[c]	ΔG_{TRP}[d]	ΔG_{PT}
CH_3O	CH_3O	69.9	−47.1	70.3	53.1	−17.2
CH_3	CH_3	69.2	−44.7	68.0	53.3	−14.7
CH_3O	H	69.0	−44.7	68.0	53.3	−14.7
CH_3	H	69.2	−43.5	66.8	53.4	−13.4
H	H	69.2	−42.6	65.9	53.5	−12.4
F	H	—[e]	−42.2	65.4	53.6	−11.8
Cl	H	—	−40.7	63.5	53.4	−10.1
Cl	Cl	—	−38.6	61.9	53.3	−8.6

[a] Ref. 44.

[b] Ref. 50.

[c] The changes in free energy for the contact radical ion pair upon the addition substituents are 4,4′-dimethoxy (4.4 kcal mol^{-1}), 4,4′-dimethyl (2.1 kcal mol^{-1}), 4-methoxy (2.1 kcal mol^{-1}), 4-methyl (0.9 kcal mol^{-1}), 4-fluoro (-0.5 kcal mol^{-1}), 4-chloro (-1.9 kcal mol^{-1}) and 4,4′-dichloro (-4.0 kcal mol^{-1}).[19]

[d] The changes in free energy for the triplet radical pair upon the addition substituents are 4,4′-dimethoxy (0.4 kcal mol^{-1}), 4,4′-dimethyl (0.2 kcal mol^{-1}), 4-methoxy (0.2 kcal mol^{-1}), 4-methyl (0.1 kcal mol^{-1}), 4-fluoro (-0.1 kcal mol^{-1}), 4-chloro (0.1 kcal mol^{-1}) and 4,4′-dichloro (0.2 kcal mol^{-1}).[19]

[e] No reported values.

Finally, the effect of substituents on the stability of the ketyl radical has been previously discussed and their effect is given in Table 1.[18]

The derived values for the free energy of proton transfer, ΔG_{PT}, are significantly more exergonic than those derived for the benzophenone–*N*,*N*-dimethylaniline system where the oxidation potential of *N*,*N*-dimethylaniline, $E_{\mathrm{D}}^{\mathrm{OX}} = 0.84$ V vs SCE, is very similar to that of *N*-methylacridan, $E_{\mathrm{D}}^{\mathrm{OX}} = 0.81$ V vs SCE, and therefore should have similar driving forces for proton transfer.[18] The reason for this discrepancy is that in our prior derivation of ΔG_{PT} the value of oxidation potential employed for *N*,*N*-dimethylaniline was based on an older measurement of 0.78 V.[48] Also, the estimate for the enthalpy of formation for the triplet radical pair was based on an older determination of the enthalpy for the

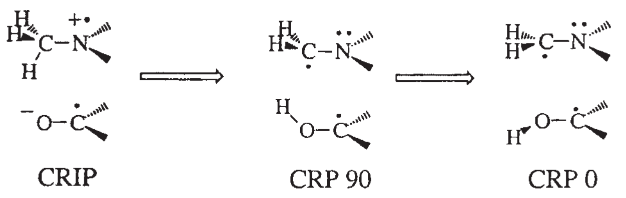

Scheme 2

addition of a hydrogen atom to the triplet state of benzophenone, $-104\,\mathrm{kcal\,mol^{-1}}$,[49] while a more accurate and recent measurement places this value at $-110.8\,\mathrm{kcal\,mol^{-1}}$.[46] These assumptions led to an underestimate of the driving force for proton transfer by approximately $-7\,\mathrm{kcal\,mol^{-1}}$ for all of the systems studied in Refs 18–20.

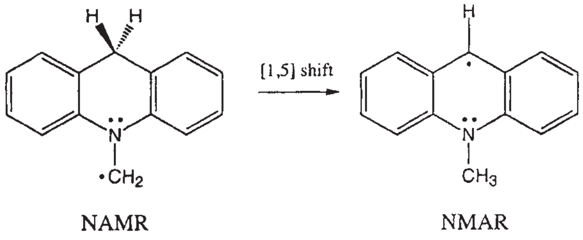

Scheme 3

Transient absorption spectra

The reaction pathway for these kinetic studies involves the formation of the first excited singlet state of substituted benzophenones, which then intersystem crosses to the triplet state on a time-scale of less than 10 ps. The triplet is quenched by electron transfer from the amine to form the triplet radical ion pair, which then decays through proton transfer forming a triplet radical pair. It is important for the kinetic analysis that the rate of formation of the triplet contact radical ion pair from the triplet state of benzophenone be fast relative to the proton transfer event and that the reactive species is indeed the triplet contact radical ion pair.

A possible concern that arises from the analysis of the energetics of the various contact radical ion pairs is energy of the triplet states of the substituted benzophenones are close in energy to the ion pair energies (Table 1). For example, the energy of 4,4′-dimethoxybenzophenone–*N*-methylacridan contract radical ion pair is estimated to be $70.3\,\mathrm{kcal\,mol^{-1}}$ above the ground-state reactants whereas the triplet-state energy of 4,4′-dimethoxybenzophenone is $69.9\,\mathrm{kcal\,mol^{-1}}$.[44] Given the uncertainty in the determination of the ion pair energies, it is necessary to establish the nature of the reacting species engaged in proton transfer.

The transient absorption spectrum at 50 ps and 1 ns following the 355 nm irradiation of 0.02 M benzophenone–0.3 M *N*-methylacridan in benzene is shown in Fig. 1. At 50 ps there is a broad absorption spanning 600–750 nm which is not present in benzophenone in the absence of *N*-methylacridan. Also present at early time is the spectrum of the triplet state of benzophenone, $\lambda_{max} = 525$ nm. Based on earlier studies, the broad absorption band is attributed to the superposition of the absorption spectrum of the radical anion of benzophenone, $\lambda_{max} = 720$ nm, and the absorption spectrum of the radical cation of *N*-methylacridan, $\lambda_{max} = 640$ nm.[37] The contact ion pair decays on the 400 ps time-scale to form the radical species absorbing between 520 and 545 nm (Fig. 1). The absorption at 545 nm has previously been assigned to ketyl radical of benzophenone.[37] The assignment of the 520 nm species is more problematic.[39] The carbon center radical associated with the removal of a hydrogen atom from the *N*-methyl group of *N*-methylacridan is not expected to absorb in the visible region as the carbon center radical formed from the removal of hydrogen atom from the *N*-methyl group of *N*-methyldiphenylamine does not display a visible absorption spectrum.[48] In the past, we have speculated that the molecular species formed on proton transfer to the radical anion of the ketone, the *N*-acridanyl methyl radical (NAMR), undergoes a facile [1,5] hydrogen shift on the 400 ps time-scale (Scheme 3) to produce radical center at the 9-position, the *N*-methylacridan-9-yl radical (NMAR); it is this species which absorbs at 520 nm.[39] A more in-depth discussion of this rearrangement and the isotopic studies supporting this proposal can be found in Ref. 39.

The transient absorption spectrum at 50 ps and 1 ns following the 355 nm irradiation of 0.02 M 4,4′-dimethoxybenzophenone–0.3 M *N*-methylacridan in benzene is shown in Fig. 2. At 50 ps, present are the triplet state of 4,4′-dimethoxybenzophenone, $\lambda_{max} = 550$ nm, and a

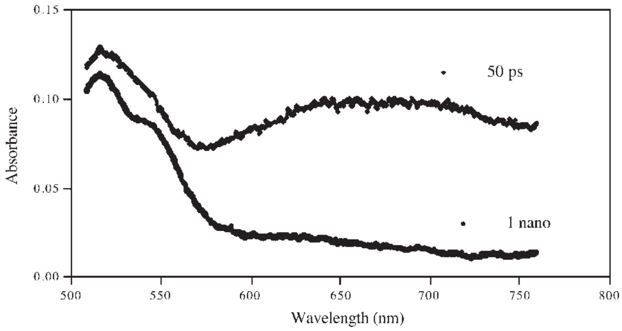

Figure 1. Transient absorption spectrum at 50 ps (top curve) and at 1 ns (bottom curve) following 355 nm irradiation of 0.02 M benzophenone–0.3 M *N*-methylacridan in benzene

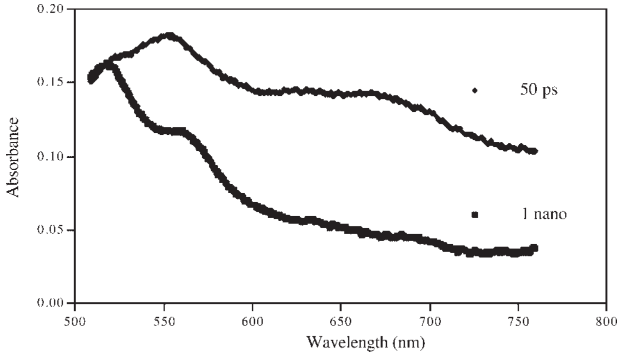

Figure 2. Transient absorption spectrum at 50 ps (top curve) and at 1 ns (bottom curve) following the 355 nm irradiation of 0.02 M 4,4′-dimethoxybenzophenone–0.3 M *N*-methylacridan in benzene

Table 2. Rate constants for proton transfer, k_{pt}, from *N*-methylacridan, rate constants for deuteron transfer, k_{dt}, from *N*-methyl-d_3-acridan and the kinetic deuterium isotope effects, k_{pt}/k_{dt}

Compound		*N*-Methylacridan	*N*-Methyl-d_3-acridan	
4	4′	k_{pt} ($\times 10^9$ s^{-1})[a]	k_{dt} ($\times 10^9$ s^{-1})	k_{pt}/k_{dt}
CH_3O	CH_3O	1.32	1.15	1.15
CH_3	CH_3	1.87	1.55	1.21
CH_3O	H	1.74	1.57	1.11
CH_3	H	2.27	1.67	1.36
H	H	2.47	1.94	1.27
F	F	2.66	1.90	1.40
Cl	H	2.77	1.69	1.64
Cl	Cl	2.45	1.35	1.82

[a] Estimated uncertainties in rate constants ± 10% (1σ).

broad spectrum extending from 600 to 750 nm, which we assign to the radical cation of *N*-methylacridan, $\lambda_{max} = 640$ nm, and the radical anion of 4,4′-dimethoxybenzophenone, $\lambda_{max} = 690$ nm.[50] By 1 ns, the two radical species are observed: the ketyl radical, $\lambda_{max} = 560$ nm, and *N*-acridanyl methyl radical, $\lambda_{max} = 520$ nm.[50] These experiments lead us to conclude that it is the contact radical ion pair that is giving rise to the triplet radical pair through proton transfer.

Kinetics

The dynamics of proton–deuteron transfer from *N*-methylacridan and *N*-methyl-d_3-acridan radical cations to the various 4,4′-substituted benzophenone radical anions in benzene were monitored at 680 nm following 355 nm excitation, the results of which are given in Table 2. The magnitude of the kinetic deuterium isotope effect ranges from 1.1 to 1.8. An example of the kinetic data for proton–deuteron transfer from *N*-methylacridan and *N*-methyl-d_3-acridan radical cations to the benzophenone radical anion is shown in Fig. 3. The residual absorption at 680 nm at long times is attributed to the absorption of radical products (Fig. 1). When *N*-methylacridan-9,9-d_2 was employed in the kinetic studies with each of the 4,4′-substituted benzophenones, a kinetic deuterium isotope effect was not observed, again supporting the proposition that the transferring proton is derived from the *N*-methyl group. An example of the kinetic data for 4,4′-dimethoxybenzophenone–*N*-methylacridan-9,9-d_2 is shown in Fig. 4.

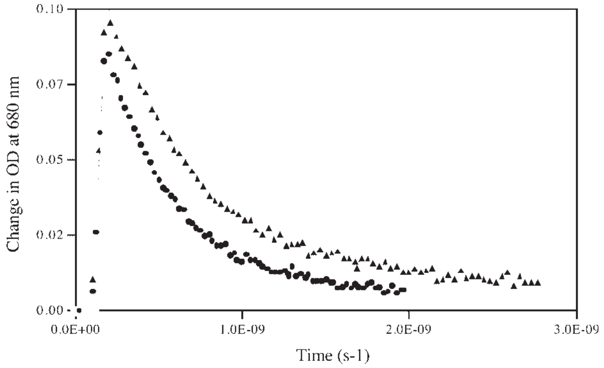

Figure 3. Transient absorption at 680 nm following 355 nm excitation of 0.02 M benzophenone in the presence of 0.3 M *N*-methylacridan (circles) and 0.3 M *N*-methyl-d_3-acridan (triangles) in benzene. Fits (solid lines) to *N*-methylacridan, $k_{pt} = 2.47 \times 10^9$ s^{-1}, and to *N*-methyl-d_3-acridan data, $k_{dt} = 1.94 \times 10^9$ s^{-1}, with pulse width 19 ps and $t_0 = 95$ ps. See Ref. 41 for data analysis

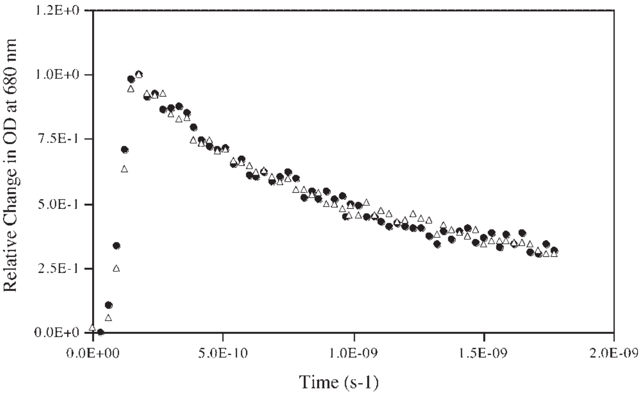

Figure 4. Normalized transient absorption at 680 nm following 355 nm excitation of 0.02 M 4,4′-dimethoxybenzophenone in the presence of 0.3 M *N*-methylacridan (filled circles) and 0.3 M *N*-methylacridan-9,9-d_2 (open triangles) in benzene

Vibrational analysis

In the following analysis of the kinetic data within the context of the Lee–Hynes model, the vibrational frequencies of the active reactant and product modes are required. The analysis assumes that the geometry of the reactive species is that depicted in Scheme 2, CRP 90. Two vibrations in the product state that are potentially active are the C—O—H in-plane bending mode, with a frequency of 768 cm^{-1}, and the O—H stretching mode, with a frequency of 2386 cm^{-1}; both vibrational frequencies were calculated at the pBP/DN** level. In the reactant state the only vibration assumed to be active is the C—H stretch with a calculated value of 2701 cm^{-1}.

DISCUSSION

The Lee–Hynes model for non-adiabatic proton transfer has been described previously.[20,36] Assuming that the dominant reaction channel is a non-adiabatic process, tunneling requires that the reactant and product states be in resonance. Resonance is achieved by the fluctuation in the solvent structure surrounding the reacting species and the energy required to reorganized the solvent structure is E_s. Another molecular motion critical in determining the dynamics of proton transfer is the low-frequency vibration Q that modulates the distance between the two heavy atoms that bound proton transfer. As the vibration reduces the distance for tunneling, the rate of tunneling increases exponentially; the relationship is given by[36]

$$C(Q) = C_0 \exp(-\alpha \Delta Q) \tag{2}$$

where C_0 is the tunneling rate at the equilibrium position of the vibrational amplitude and ΔQ measures the displacement distance of the low-frequency vibration. The sensitivity of the tunneling rate to ΔQ is measured by the parameter α, which for proton transfer ranges in value from 25 to 35 Å^{-1}.[27] This phenomenon produces an energy term E_α reflecting the coupling of the proton reaction coordinate to the Q vibration. The relationship between α and E_α is given by $E_\alpha = h^2 = \alpha/2m$, where m is the reduced mass associated with the low-frequency vibration.

Within Lee–Hynes theory, the rate constant for non-adiabatic proton transfer from the n_R vibrational level in the reactant state to the m_P vibrational level of the product state is given by[36]

$$k(n_R \rightarrow m_P) = k_{m_P},\, n_R(0)(\pi/2A_2)^{1/2} \exp(-A_1^2/2A_2) \tag{3}$$

where $k_{m_P,n_R}(0), A_1$ and A_2 are defined as

$$\begin{aligned} k_{m_P,n_R}(0) = {} & 2(2\pi/h)^2[C_{m_P,n_R}(Q)]2 \\ & \times \exp[(E_\alpha/h\omega_Q)\, 2\coth(\beta h\omega_Q/2)] \end{aligned}$$

$$\begin{aligned} A_1 = {} & (2\pi/h)\{\Delta E + E_s + E_Q + E_\alpha + [hm_P\omega_P - hn_R\omega_R] \\ & + 2\Delta Q/|\Delta Q|(E_\alpha E_Q)^{1/2}\coth(\beta h\omega_Q/2)\} \end{aligned}$$

$$\begin{aligned} A_2 = {} & 2(2\pi/h)^2 k_B T\{E_s + (E_\alpha + E_Q)(\beta h\omega_Q/2\pi \coth \\ & \{\beta h\omega_Q/2\pi\} + \Delta Q/|\Delta Q|(E_\alpha E_Q)^{1/2}(\beta h\omega_Q)\} \end{aligned}$$

with the terms defined as follows:

ω_R = vibrational frequency of the reactant state
ω_P = vibrational frequency of the product state
ΔQ = distance change in the intermolecular separation on going from the reactant state to the product state
E_Q = the energy change associated with ΔQ
$C_{m_P,n_R}(Q)$ = the tunneling matrix element from nth level in reactant state to mth level in the product state
ΔE = free energy change for reaction.

Within the WKB approximation, the tunneling term $C_{m_P,n_R}(Q)$ is given by[36]

$$\begin{aligned} C_{m_P,n_R}(Q) = {} & (h/4\pi^2)(\omega_R\omega_P)^{1/2}\exp\{-2\pi^2/h\omega^\ddagger \\ & [V^\ddagger - 1/2(V_{n_R}\ V_{m_P})]\} \end{aligned} \tag{4}$$

with the following terms defined as:

$V^\ddagger$ = the potential energy maximum in proton transfer coordinate
$\omega^{\ddagger)}$ = mass-weighted frequency associated with the inverted parabola associated with $V^\ddagger$
V_{n_R} = energy of the reactant state
V_{m_P} = energy of the product state.

The Lee–Hynes model for non-adiabatic proton transfer is also applicable for non-adiabatic deuteron transfer. Within the Born–Oppenheimer approximation, the parameters affected upon replacement of a proton by a deuteron are the zero-point energies of the reactant and product states and the mass-weighted frequency $\omega^\ddagger$, each being reduced by a factor of $1/\sqrt{2}$. Furthermore, since the rate of tunneling depends on α, which is determined by the fall-off of the tails of the wavefunction associated with the transferring particle, replacing a proton by a deuteron leads to an in increase α for the deuteron (α_D) relative to α for the proton (α_H), where $\alpha_D = \sqrt{2}\alpha_H$ (J. T. Hynes, personal communication). Deuterium substitution thus increases E_α for deuteron transfer by a factor of 2 relative to E_α for proton transfer.

In applying the Lee–Hynes model in the analysis of the correlation of the rate constants for proton–deuteron transfer with driving force, several assumptions are made for the value of the parameters controlling the rates of transfer. For the present analysis, we assume that proton–deuteron transfer does not significantly change the intermolecular separation of the reacting species so that if $\Delta Q = 0$, then $E_Q = 0$. The value for E_α for proton transfer is set to $1.0\,\text{kcal}\,\text{mol}^{-1}$; the procedure for the estimation of E_α can be found in Ref. 27. Also, in the absence of experimental data for vibrational frequencies for contact radical ion pairs, the value of the vibrational frequency for the promoting mode Q is set to $200\,\text{cm}^{-1}$. The barrier frequency $\omega^\ddagger$ is also unknown, and we therefore adopt the value of $2500\,\text{cm}^{-1}$ that was derived from hydrogen atom transfer study of Lee and Hynes.[36] In the fitting procedure, the parameters $\omega^\ddagger$ and $V^\ddagger$ are highly correlated so that the derived value of $V^\ddagger$ will depend on the assumed value for $\omega^\ddagger$.

The remaining terms found in the Lee–Hynes model are the barrier height $V^\ddagger$ and the solvent reorganization energy E_s, both of which serve as fitting parameters. In the present model that we employ, there are two reaction paths, transfer to the stretch and to the bend of the product state, CRP 90. Each reaction path has its own value for $V^\ddagger$; however, at present we assume that they are same. Fitting the model to the correlation of the experimental rate constants for proton transfer with the free energy change for reaction, the derived values for $V^\ddagger$ and E_s are $V^\ddagger = 21.0\,\text{kcal}\,\text{mol}^{-1}$ and $E_s = 11.5\,\text{kcal}\,\text{mol}^{-1}$ (Fig. 5). Over the range in driving force of -8 to $-17.5\,\text{kcal}\,\text{mol}^{-1}$, there is a good correlation between the model and the experiment. At large driving force,

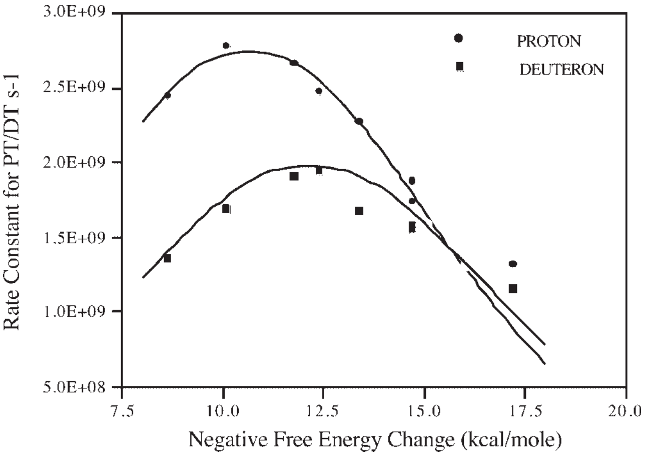

Figure 5. Plot of the experimental rate constants for proton transfer from *N*-methylacridan cation radical and deuteron transfer from *N*-methyl-d_3-acridan cation radical versus negative free energy change in benzene. Circles, experimental data for proton transfer; squares, experimental data for deuteron transfer. The solid curve for proton transfer comes from the Lee–Hynes model with $E_\alpha = 1.0\,\text{kcal mol}^{-1}$, $V^\ddagger = 21.0\,\text{kcal mol}^{-1}$, $\omega_Q = 200\,\text{cm}^{-1}$, $E_S = 11.5\,\text{kcal mol}^{-1}$, $\Delta Q = 0.0$ Å, $E_Q = 0.0\,\text{kcal mol}^{-1}$, $\omega_R = 2701\,\text{cm}^{-1}$, ω_P for $m(0) = 768\,\text{cm}^{-1}$ (bend), ω_P for $m(1) = 2386\,\text{cm}^{-1}$ (stretch) and $\omega^\ddagger = 2500\,\text{cm}^{-1}$. The solid curve for deuteron transfer comes from the Lee–Hynes model with $E_\alpha = 2.0\,\text{kcal mol}^{-1}$, $V^\ddagger = 22.0\,\text{kcal mol}^{-1}$, $\omega_Q = 200\,\text{cm}^{-1}$, $E_S = 11.5\,\text{kcal mol}^{-1}$, $\Delta Q = 0.0$ Å, $E_Q = 0.0\,\text{kcal mol}^{-1}$, $\omega_R = 1910\,\text{cm}^{-1}$, ω_P for $m(0) = 543\,\text{cm}^{-1}$ (bend), ω_P for $m(1) = 1687\,\text{cm}^{-1}$ (stretch) and $\omega^\ddagger = 1768\,\text{cm}^{-1}$

$-17.5\,\text{kcal mol}^{-1}$, there is some deviation between the model and experiment, with the model underestimating the rate of proton transfer. It is in this region of the driving force that the first overtones of the O—H stretch C—O—H bend in the product state should begin to make contributions to the overall reaction rate and therefore it is not surprising that the model underestimates the rate constant for proton transfer as the overtones in the product state were not taken into account in the analysis.

In fitting the Lee–Hynes model to the kinetic data for deuteron transfer, the frequencies of the active vibrations in the reactant and product states and $\omega^\ddagger$ are scaled by a factor $1/\sqrt{2}$. E_α for deuteron transfer is increased to $2\,\text{kcal mol}^{-1}$. The variable that serves as a fitting parameter in the modeling of the deuterium kinetic data is only the barrier height $V^\ddagger$, which we define as the difference between the zero point energy of the reactant mode and the top of the electronic barrier. For proton transfer, the derived value of $V^\ddagger$ is $21.0\,\text{kcal mol}^{-1}$. If deuteration reduces the zero point energy of the transferring mode by a factor of $1/\sqrt{2}$, then the value of $V^\ddagger$ for deuteron transfer should be $22.1\,\text{kcal mol}^{-1}$. When the model is fitted to the kinetic data for deuteron transfer, the derived value for $V^\ddagger$ is $22.0\,\text{kcal mol}^{-1}$, which is remarkably close to the expected value for $V^\ddagger$.

Overall, the Lee–Hynes model for proton–deuteron transfer gives a very good account of the correlation of the rates constants for proton–deuteron transfer with driving force. Experimentally, the maximum rate of transfer shifts from $-10.5\,\text{kcal mol}^{-1}$ for proton transfer to $-12.5\,\text{kcal mol}^{-1}$ for deuteron transfer. This shift can be understood within the context of the Lee–Hynes model as reflecting an increase in E_α on replacing a proton by a deuteron. This shift points to the importance of low-frequency modes in modulating the rate of proton–deuteron tunneling. Also, the low values of the kinetic deuterium isotope effect, ranging from 1.1 to 1.8, can be understood within the context of the model. Previously, low values for the kinetic deuterium isotope effect were taken as indication that tunneling, from the Bell perspective, is not making an important contribution to the overall rate of reaction. However, in the Lee–Hynes theory, which is exclusively a tunneling model, low values of the kinetic deuterium isotope effect can be expected.

The most remarkable feature of the present kinetic data is the existence of an inverted region, that is, with an increase in driving force, the rate of transfer decreases. Similar behavior is also observed for benzophenone–*N*,*N*-dimethylaniline and benzophenone–*N*,*N*-diethylaniline systems.[18,19] Transition-state theory and variational transition-state theory, even with the inclusion of tunneling in the vicinity of the transition state, cannot account for the kinetic behavior of the inverted region.[23] For these models, the rate of proton–deuteron transfer will initially increase with increasing driving force and finally reach a limiting value. Only a non-adiabatic model that incorporates the critical solvent coordinate can produce an inverted region.

A note of caution is in order. The benzophenone–*N*-methylacridan is a rather unusual contact radical ion pair owing to the π-stacked nature of the complex. The π-stacking leads to a constraint in the distance of approach of the two heavy atoms that bound the proton–deuteron transfer. This distance, which is of the order of 3.3 Å, places the transfer process in the non-adiabatic regime. If the constraint in distance were relaxed, allowing the close approach of the two heavy atoms, the reaction process may then move into the adiabatic regime, where the electronic barrier in the transfer coordinate drops below the zero point energy of the transferring mode. In the adiabatic regime, the correlation of the rate constant of proton–deuteron transfer with driving force leads to an initial increase in rate of transfer with driving force, but then levels out to a constant value; an inverted region is not predicted for adiabatic transfer.[51] Such kinetic behavior has been observed in the dynamic studies of naphthol photoacids with carboxylic base pairs in water.[9,10] Most bimolecular proton transfer processes in solution will probably proceed by an adiabatic process unless there is an unusual constraint such as a steric effect or π-stacking. In enzymatic systems with pre-organization leading to constraints in distances for transfer, non-adiabatic proton–deuteron transfer may be important reaction processes.[52–56]

Finally, attention is drawn to the recent report of Andrieux *et al.*, who observed an inverted region in proton transfer to the diphenylmethyl anion.[57] This kinetic behavior would imply that the mechanism of proton transfer is through a non-adiabatic process.

Acknowledgment

This work was supported by grants from the National Science Foundation, CHE-0408265.

REFERENCES

1. Anne A, Hapiot P, Moiroux J, Neta P, Saveant JM. *J. Am. Chem. Soc.* 1992; **114**: 4694–4701.
2. Barbara PF, Walsh PK, Brus LE. *J. Phys. Chem.* 1989; **93**: 29–34.
3. Lawrence M, Marzzacco C, Morton C, Schwab C, Halpern AM. *J. Phys. Chem.* 1991; **95**: 10294–10299.
4. Tolbert LM, Nesselroth SM. *J. Phys. Chem.* 1991; **95**: 10331–10336.
5. Moog RS, Maroncelli M. *J. Phys. Chem.* 1991; **95**: 10359–10369.
6. Robinson GW. *J. Phys. Chem.* 1991; **95**: 10386–10391.
7. Shida N, Almlof J, Barbara PF. *J. Phys. Chem.* 1991; **95**: 10457–10464.
8. Pines E, Fleming GR. *J. Phys. Chem.* 1991; **95**: 10448–10457.
9. Pines E, Fleming GR. *Chem. Phys.* 1994; **183**: 393–402.
10. Pines E, Magnes B, Lang MJ, Fleming GR. *Chem. Phys. Lett.* 1997; **281**: 413–420.
11. Zewail AH. *J. Phys. Chem.* 1996; **100**: 12701–12724.
12. Hineman MF, Bruker GA, Kelley DF, Bernstein ER. *J. Chem. Phys.* 1990; **92**: 805.
13. Syage JA. *J. Phys. Chem.* 1995; **99**: 5772–5786.
14. Brucker GA, Swinney TC, Kelley DF. *J. Phys. Chem.* 1991; **95**: 3190–3195.
15. Swinney TC, Kelley DF. *J. Chem. Phys.* 1993; **99**: 211–221.
16. Parsapour F, Kelley DF. *J. Phys. Chem.* 1996; **100**: 2791–2798.
17. Peters KS. In *Advances in Photochemistry*, vol. 27, Neckers DC (ed). Wiley: New York, 2002; 51–82.
18. Peters KS, Cashin A, Timbers P. *J. Am. Chem. Soc.* 2000; **122**: 107–113.
19. Peters KS, Cashin A. *J. Phys. Chem. A.* 2000; **104**: 4833–4838.
20. Peters KS, Kim G. *J. Phys. Chem. A* 2001; **105**: 4177–4181.
21. Bell RP. *The Tunnel Effect in Chemistry.* Chapman and Hall: London, 1980.
22. Bell RP. *The Proton in Chemistry.* Chapman and Hall: London, 1973.
23. Truhlar DG, Garrett BC. *Acc. Chem. Res.* 1980; **14**: 440.
24. Truhlar DG, Gordon MS. *Science* 1990; **249**: 491–498.
25. Kuznetsov AM. *Charge Transfer in Physics, Chemistry and Biology.* Gordon and Breach: Luxembourg, 1995.
26. Kuznetsov AM, Ulstrup J. *Can. J. Chem.* 1999; **77**: 1085–1096.
27. Borgis DC, Lee S, Hynes JT. *Chem. Phys. Lett.* 1989; **162**: 19–26.
28. Borgis D, Hynes JT. *The Enzyme Catalysis Process*. Plenum Press: New York, 1989.
29. Borgis D, Hynes JT. *J. Chem. Phys.* 1991; **94**: 3619–3628.
30. Borgis D, Hynes JT. *J. Phys. Chem.* 1996; **100**: 1118–1128.
31. Cukier RI, Morillo M. *J. Chem. Phys.* 1989; **91**: 857–863.
32. Li D, Voth GA. *J. Phys. Chem.* 1991; **95**: 10425–10431.
33. Lobaugh J, Voth GA. *J. Chem. Phys.* 1994; **100**: 3039–3047.
34. Hammes-Schiffer S, Tully JC. *J. Chem. Phys.* 1994; **101**: 4657–4667.
35. Hammes-Schiffer S. *Acc. Chem. Res.* 2001; **34**: 273–282.
36. Lee S, Hynes JT. *J. Chim. Phys* 1996; **93**: 1783–1807.
37. Peters KS, Pang E, Rudzki J. *J. Am. Chem. Soc.* 1982; **104**: 5535–5538.
38. Manring LE, Peters KS. *J. Am. Chem. Soc.* 1983; **105**: 5708–5709.
39. Manring LE, Peters KS. *J. Am. Chem. Soc.* 1985; **107**: 6452–6458.
40. Birks JB. In *The Exciplex*, Gordon M, Ware WR (eds). Academic Press: New York, 1975; 39–73.
41. Peters KS, Lee J. *J. Phys. Chem.* 1993; **97**: 3761–3764.
42. Hehre WJ, Yu J, Klunzinger PE, Lou L. *A Brief Guide to Molecular Mechanics and Quantum Chemical Calculations*. Wavefunction: Irvine, CA, 1998.
43. Arnold BR, Farid S, Goodman JL, Gould IR. *J. Am. Chem. Soc.* 1996; **118**: 5482–5483.
44. Leigh WJ, Arnold DR, Humphreys RWR, Wong PC. *Can. J. Chem.* 1980; **58**: 2537–2549.
45. Parker VD, Tilset M. *J. Am. Chem. Soc.* 1991; **113**: 8778–8781.
46. Arnaut LG, Caldwell RA. *J. Photochem. Photobiol. A: Chem.* 1992; **65**, 15–20.
47. Dombrowski GW, Dinnocenzo JP, Farid S, Goodman JL, Gould IR. *J. Org. Chem.* 1999; **64**: 427–432.
48. Miyasaka H, Morita K, Kamada K, Mataga N. *Bull. Chem. Soc. Jpn.* 1990; **63**: 3385–3397.
49. Walling C, Gibian MJ. *J. Am. Chem. Soc.* 1965; **87**: 3361–3364.
50. Peters K, Kim G. *J. Phys. Chem. A* 2004; **108**: 2598–2606.
51. Kiefer PM, Hynes JT. *J. Phys. Chem. A* 2003; **107**: 9022–9039.
52. Kohen A, Klinman JP. *Acc. Chem. Res.* 1998; **31**: 397–404.
53. Rucker J, Klinman JP. *J. Am. Chem. Soc.* 1999; **121**: 1997–2006.
54. Antoniou D, Schwartz SD. *Proc. Natl. Acad. Sci. USA* 1997; **94**: 12360–12365.
55. Caratzoulas S, Mincer JS, Schwartz SD. *J. Am. Chem. Soc.* 2002; **124**: 3270–3276.
56. Alhambra C, Corchado JC, Sanchez ML, Gao J, Truhlar DG. *J. Am. Chem. Soc.* 2000; **122**: 8197–8203.
57. Andrieux CP, Gamby J, Hapiot P, Saveant JM. *J. Am. Chem. Soc.* 2003; **125**: 10119–10124.